Materials Science & Engineering A 616 (2014) 189–195

Contents lists available at ScienceDirect

Materials Science & Engineering A

journal homepage: www.elsevier.com/locate/msea

Serration behavior and shear band characteristics during tensile deformation of an ultrafine-grained 5024 Al alloy

M. Komarasamy, R.S. Mishra *

Department of Materials Science and Engineering and Center for Friction Stir Processing, University of North Texas, Denton, TX 76203, USA

ARTICLE INFO

Article history:
Received 1 June 2014
Received in revised form
7 August 2014
Accepted 8 August 2014
Available online 17 August 2014

Keywords:
Mechanical characterization
Micromechanics
Dislocations
Shear bands
Fracture

ABSTRACT

The main objective of this work is to understand the major deformation mechanisms operative in the entire plastic strain regime of an ultrafine-grained (UFG) 5024 Al alloy. The initial microstructure in both coarse-grained (CG) and UFG conditions was characterized by transmission electron microscopy and orientation imaging microscopy to better correlate the observed deformation behavior with the microstructural elements. The engineering stress–strain curves in both CG and UFG conditions were serrated from onset of yielding to the point of sample failure although the net intensity of the serrations varied in both the conditions. Interrupted tensile testing with corresponding surface analysis using scanning electron microscopy (SEM) was carried out to clearly demarcate the micro-mechanisms operative in various plastic strain regimes. The serration amplitude as a function of time in UFG material was studied and displayed a different behavior when compared with CG material. The reason for higher non-uniform elongation has been explained in terms of micron-sized shear bands and void coalescence mechanism. Dislocation slip was observed to be the major strain accommodation mechanism, along with shear bands and grain rotation. Analysis of failed specimen surfaces using SEM further assisted in understanding and quantifying the damage accumulation and failure mechanism.

1. Introduction

Ultra-fine grained (UFG) materials have become well known because of outstanding tensile strength properties [1–3], based on Hall–Petch relationship and its possible ways of production through severe plastic deformation (SPD) techniques. Various SPD techniques have been developed, which are equal channel angular extrusion/pressing (ECAE/P) [4], accumulated roll bonding (ARB) [5], high pressure torsion (HPT) [4], multiple-forging (MF) [4], cryorolling (CR) [6] and friction stir processing (FSP) [7]. The mechanism of UFG production in ECAP and HPT is the introduction of large strain into the material, which results in high defect concentration, especially high density of dislocations, and non-equilibrium nature of grain boundaries [4,5]. In general, the ductility mainly depends on the work hardening ability of the material. The presence of large dislocation density in SPD materials limits further dislocation storage and moreover, the fine grains have very limited ability to store intragranular dislocations. Although UFG materials possess impressive tensile strength properties, their use as structural component is limited by its low ductility. The ductility of UFG materials produced via SPD techniques like ECAP, CR, etc., has been increased through the following ways [8,9], introduction of bi-modal grain size distribution, annealing treatment to relieve internal stress, by the introduction of nano-sized precipitates, by testing at higher strain rates or at lower temperature to avoid dynamic recovery. Sabirov et al. [10] proposed another technique where the increased ductility in the lower strain rate regime was attributed to the activation of micron-sized shear bands instead of macro ones. FSP, a variant of friction stir welding (FSW), was a relatively new addition to the SPD techniques and was first introduced by Mishra et al. [7]. FSP is a proven technique for microstructural modification and grain refinement in various Al and Mg alloys [11,12]. The details on FSP can be found elsewhere [7]. The resultant microstructure obtained from FSP has lower dislocation density, high fraction of high angle grain boundaries (HAGB) and fine grain size [13].

Strain softening, a decrease in strength with increasing plastic strain, was observed in most of the UFG material under tensile loading conditions [10,14,15]. This has been attributed to the limited ability of the material to store dislocations, localization in the form of shear bands and neck formation. A number of mechanisms have been proposed for the formation and propagation of SBs under both static and cyclic straining conditions [16–18]. Based on the static tests performed on Fe, Jia et al. [18] proposed that the large soft grains initiated the shear bands and the bands propagated by the reorientation of the smaller grains surrounding the large grain. Other than strain softening, strain rate softening is another instability

* Corresponding author. Tel.: +1 940 565 2316; fax: +1 940 565 4824.
E-mail address: Rajiv.Mishra@unt.edu (R.S. Mishra).

http://dx.doi.org/10.1016/j.msea.2014.08.027

that was observed in solid solution strengthened alloys which could potentially affect the formability. The observation of serrations in the stress–strain curve is the indication of the instability that stems from the Portevin–Le Chatelier (PLC) activity. Strain rate softening is the result of the dynamic interaction between the diffusing solutes and the mobile dislocations that are temporarily arrested at obstacles, such as forest dislocations [19,20]. The serrations were observed in a particular strain rate and temperature regime [21]. For the conventional grain size regime, both the serration amplitude and the frequency increased with decreasing grain size [22]. From the studies of Tabata et al. [23] and Klose et al. [24], the serrations were not just due to solute–dislocation interaction, but also due to the dislocation pile up at the obstacles and its breakaway from that obstacle at an increased stress.

Since the microstructure obtained from each of the SPD techniques differs in dislocation density, grain/cell size, and in the grain boundary character distribution, it is vital to understand the deformation behavior of the UFG materials produced by various SPD techniques. In this study, a detailed analysis was made to understand the deformation mechanisms operative in various regimes of a stress–strain in UFG Al–Mg–Sc alloy produced via FSP. There are no systematic reports on the tensile deformation behavior of the UFG Al–Mg–Sc alloy produced by FSP. Throughout the study, wherever applicable comparisons with CG tensile behavior were made to understand how the underlying deformation mechanisms change with grain size.

2. Experimental procedure

The material used in this study was 5024 Al alloy (Al–Mg–Sc) in H116 tempered condition and the plates were ~6 mm in thickness. A single pass FSP was carried out on this plate to produce UFG microstructure. The FSP tool used for processing had a conical pin with step-spiral profile, concave shoulder and was made of tool steel. The pin height, pin diameter at the root and tip, and the shoulder diameter of the FSP tool were 2.25 mm, 6.00 mm, 3.75 mm and 12.00 mm, respectively. The schematic of the FSP tool used to obtain UFG microstructure is shown in Fig. 1a. The following FSP processing parameters were used for this study: tool rotation rate of 325 revolutions per minute, tool traverse speed of 203.2 mm/min, the tool tilt angle of 2.5° and the target depth of 2.35 mm. FSP was carried out along the rolling direction of the as-received plate.

The grain size, grain size distribution (GSD) and the fraction of HAGB were measured using electron back scattered diffraction (EBSD) system installed in a FEI Nova NanoSEM 230 with field emission gun electron source. The samples for EBSD analysis were polished down to 1 μm surface finish using diamond polishing solution and then to 0.02 μm surface finish using colloidal silica suspension. Since the grain size was expected to be of few hundreds of nanometers, a step size of 0.08 μm was used for EBSD data collection.

Samples for TEM were first thinned down to 100 μm through mechanical polishing, and then 3 mm disks were punched out from the sheet. The disks were further thinned down using the dimpling method, and the final thinning was done using precision ion polishing system.

Samples for tensile testing were taken along FSP direction. The following were the dimensions of the rectangular mini-tensile specimen gage section tested: gage length of 5 mm, width of ~1.23 mm, and thickness of ~1.10 mm. A schematic of mini-tensile specimen is shown in Fig. 1b. The samples were polished until 0.05 μm surface finish and then cleaned properly before tensile testing. Then, a few scratches were introduced deliberately on the polished surface. Tensile testing was done using a custom-built computer controlled mini-tensile testing machine. The tests were carried at an initial strain rate of $1 \times 10^{-3}\ s^{-1}$ and at room temperature. The cross head velocity (gage length × initial strain rate) was maintained constant throughout the tensile test. The load–displacement data of the tensile test was recorded using National Instruments data acquisition card at a frequency of 60 Hz to capture detailed load response.

Interrupted tensile tests at the same test conditions mentioned above were done with surface analysis after each step using SEM in a secondary electron mode. The fractured surface was also analyzed using SEM.

3. Results

3.1. Microstructural characterization

The CG material was analyzed by both OIM and TEM to better understand the initial microstructure, and UFG material was analyzed under OIM to quantify the grain size, GSD and misorientation angle distribution. The rolled microstructure and the presence of Al_3Sc particles are shown in Fig. 2.

The as-received material was severely rolled, had elongated grains and predominantly had (101) orientation of planes, as can be seen

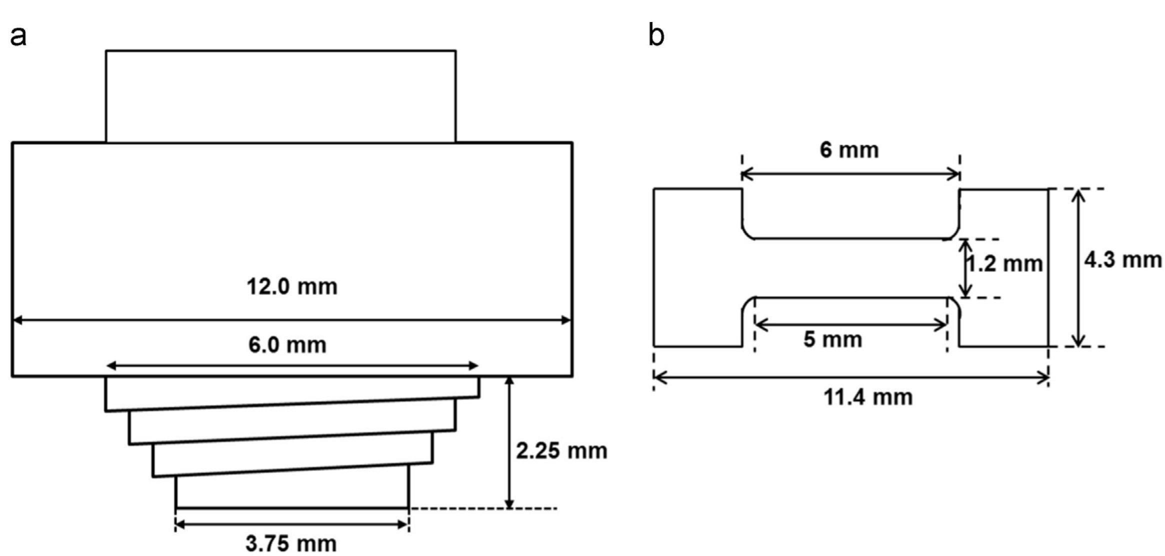

Fig. 1. Schematic of (a) FSP tool used to obtain UFG microstructure and (b) mini-tensile specimen is shown.